O atom due to charge transfer.

Conclusion

From the large electron density deficit between the oxygens and the weak electron density accumulation in the centers of the N-N, C-O, and C-N bonds and other features in the standard deformation density for 1,2,7,8-tetraaza-4,5,10,11-tetraoxatricyclo[6.4.1.1]tetradecane, one might infer that there might be deficiencies in the theory of covalent bonds. However, the features are due to the choice of a spherical-atom promolecule. Although the spherical-atom promolecule has important advantage for the experimentalist, all partitioning schemes, ours included, are arbitrary. However, the standard deformation density can be difficult to interpret without some additional "tools". To begin with, for electronegative atoms with more than half-filled shells, such as oxygen, the changes in the electron density due to the formation of the O-O single chemical bond are masked by the atomic orientation of O in the promolecule. Here, orientation of the O atoms in the promolecule improves the situation, and is particularly important because it has a dramatic effect on the density difference but does not change the energy.

The subtraction of any promolecule is useful only if it reveals features related to chemical concepts that are not visible in the total density. Here we have revealed features which are meaningful for chemists by using the chemical concept of a valence-state atom. We have partitioned the standard deformation density for this molecule into two parts corresponding to the often dominant change in density in preparation for bonding (atomic orientation of ground-state spherical O atoms and then promotion, polarization, and hybridization of all the atoms) and the smaller change in density due to covalent bond formation (constructive interference and charge transfer between valence-state optimum hybrids). Also, using these "prepared-for-bonding atoms", we isolated each bond from the complex difference density as a difference density of the two-electron bond. For the O-O and N-N bonds, the difference densities of covalent bond formation reveal not only the strong accumulation of charge in the internuclear region but also the concomitant depletion of charge in the nonbonding regions beyond the nuclear centers along the bond axis which together are the signature of the covalent bond. For the C-O and C-N bonds, similar maps show the correct direction of loss and gain of density due to charge transfer in these polar covalent bonds. The N is atypical because the strain causes the lone pair to contain more p character than an unstrained lone pair.

Thus, the unexpected features are explicable. One easily sees why the electron density in covalent bonds may appear weak or absent and why the patterns of gain and loss of density appear opposite that expected when two spherical atoms form a bond. The standard deformation densities of C-C and C-H bonds in typical organic molecules show quite large accumulations of density, since the density of the usual spherical atom reference is much closer to that of the valence state for C and H than it is for atoms which have lone pairs like O and N.

Is there a relationship between the standard deformation density of a bond and the strength of the bond? No, not even qualitatively. Is there a choice of promolecule for which there would be a simple direct relationship? A promolecule made from simple oriented ground-state atoms would not work since hybridizations and especially charge transfer can mask the constructive interference. For different bonds, the deformation density is not proportional to bond strength. Our partitioning scheme has potential, but is limited because even here charge transfer can mask constructive interference.

Acknowledgment. The authors gratefully acknowledge the support of the National Science Foundation. Grant No. CHE 83-09936 and CHE 86-19420 supported this work and Grant No. CHE 80-15792 assisted in the purchase of the VAX 11/780.

Registry No. 1,2,7,8-Tetraaza-4,5,10,11-tetraoxatricyclo[6.4.1.1]tetradecane, 81286-97-7.

Acid-Catalyzed Hydrogenation of Olefins. A Theoretical Study of the HF- and H_3O^+-Catalyzed Hydrogenation of Ethylene

Juan Carlos Siria, Miquel Duran, Agusti Lledós, and Juan Bertrán*

Contribution from the Departament de Quimica, Universitat Autònoma de Barcelona, 08193 Bellaterra, Catalonia, Spain. *Received March 11, 1987*

Abstract: The HF- and H_3O^+-catalyzed hydrogenation of ethylene and the direct addition of molecular hydrogen to ethylene have been studied theoretically by means of ab initio MO calculations using different levels of theory. The main results are that catalysis by HF lowers the potential energy barrier to a large extent, while catalysis by H_3O^+ diminishes dramatically the barrier for the reaction. Entropic contributions leave these results unchanged. The mechanisms of the two acid-catalyzed hydrogenations are somewhat different. While catalysis by HF exhibits bifunctional characteristics, catalysis by H_3O^+ proceeds via an initial formation of a carbocation. It is shown that catalysis by strong acids may be an alternate way for olefin hydrogenation.

Both hydrogenation of olefins and dehydrogenation of alkanes are reactions of great industrial importance. The molecular addition of hydrogen to ethylene is a prototype of these reactions, which is known to occur via a high-energy barrier. It has been established for a long time that the reaction proceeding via a least-motion path with a four-centered transition state is symmetry forbidden.[1] Moreover, recent theoretical calculations have shown that the barrier for a reduced symmetry path is also very high.[2] It is thus not surprising that catalysis of this reaction has been a matter of great importance in the literature.

Since the turn of the 19th century, several metal catalysts have been used successfully at different pressures and temperatures.[3]

(1) Woodward, R. B.; Hoffmann, R. *The Conservation of Orbital Symmetry*; Verlag Chemie: Weinheim, 1970.

(2) Gordon, M. S.; Truong, T. N.; Pople, J. A. *Chem. Phys. Lett.* **1986**, *130*, 245-248.

(3) Augustine, R. L. *Catalytic Hydrogenation*; Marcel Dekker: New York, 1965.

0002-7863/87/1509-7623$01.50/0

Table I. Main Bond Lengths (in Å) of the Optimized Structures of Reactants, Transition States, and Products of Reactions 1-3

	C1-C2	C1-H1	H1-H2	H2-C2	H2-X	X-H3	H3-C2
C_2H_4	1.315						
H_2			0.735				
HF						0.937	
H_3O^+						0.979	
$C_2H_4 \cdot H_2$	1.316	3.286	0.735				
TS1	1.426	1.481	1.178	1.694			
C_2H_6	1.542	1.084	3.075	1.084			
$C_2H_4 \cdot HF$	1.320					0.940	2.418
$C_2H_4 \cdot HF \cdot H_2$	1.320	4.241	0.734		2.195	0.942	2.399
TS2	1.409	1.670	0.865		1.347	1.236	1.325
$C_2H_6 \cdot HF$	1.544	1.085	3.501		0.938	2.195	1.080
$C_2H_4 \cdot H_3O^+$	1.331					1.026	2.036
$C_2H_4 \cdot H_3O^+ \cdot H_2$	1.331	4.645	0.735		2.777	1.027	2.035
TS3	1.459	1.930	0.757		1.976	2.042	1.094
$C_2H_6 \cdot H_3O^+$	1.546	1.091	1.876		0.988	2.896	1.088

Nevertheless, not until the middle of the 20th century was the mechanism of hydrogenation intensively studied. Recently, state-of-the-art techniques applied to Pt and Rh single crystals, which act as catalysts for the hydrogenation of ethylene, have shown that the reaction occurs on an active overlayer rather than a metal surface.[4] As Somorjai has stated in a recent paper, this type of reaction over heterogeneous catalysts may also occur over homogeneous catalysts.[4b] The first practical catalyst for the homogeneous hydrogenation of unsaturated hydrocarbons was reported by Wilkinson in 1956, who used the rhodium complex $Rh(PPh_3)_3Cl$.[5] The mechanism of this catalysis is at present quite well understood, even though several proposals have been made on the steps involved along the reaction.[6,7] In any case, one of the steps is accepted by all authors, where the oxidative addition of hydrogen to the metal atom is carried out; i.e., the hydrogen bond is broken by the catalyst. Therefore, the heterogeneous or homogeneous catalysis by metals proceeds by a stepwise mechanism that is very different from the mechanism of a direct addition of molecular hydrogen to ethylene.

Strong acids offer a novel method to hydrogenate hydrocarbons.[8] The main steps of the proposed mechanism consist of an initial protonation of the olefin to yield a carbocation, and the attack of a carbocation to molecular hydrogen. In this last step, the hydrogen molecule is broken, the proton is regenerated, and the hydrogenated olefin is obtained. In addition to this direct process, the reverse one, dehydrogenation of olefins, is also catalyzed by acids, for instance, H_2SO_4. The first step consists in this case of the formation of a carbocation by means of an oxidizing agent.[9] This carbocation may then lead to an olefin if a proton is lost.

Many theoretical studies of the main step of the mechanism of the heterogeneous catalysis of olefin hydrogenation, the absorption of molecular hydrogen onto the metal surface, have appeared in the last decade.[10] Some aspects of the mechanism of the homogeneous catalysis by the Wilkinson catalyst have been investigated as well.[7,11] However, no theoretical studies have been accomplished, to our knowledge, on the acid-catalyzed hydrogenation of olefins. The purpose of the present paper is to provide a deeper insight into this last type of catalytic hydrogenation, where the olefin is modeled by an ethylene molecule and HF and H_3O^+ are used as acids of different strength. Special attention is paid to three points in this paper: first, the influence of the acid strength on the formation of the carbocation; second, how breaking of the hydrogen molecule is done. Special emphasis will be laid on this aspect since it is the main point in any catalytic hydrogenation. Finally, in comparison with the uncatalyzed reaction, is the requirement that the catalyzed process must necessarily exhibit a stepwise mechanism.

Methodology

To carry out the theoretical studies in this work we employed the supermolecule model throughout. Ab initio closed-shell SCF calculations were performed with the GAUSSIAN 82[12] and MONSTERGAUSS[13] series of programs. The 3-21G[14] basis set was used for all geometry optimizations. The correlation energy of the meaningful stationary points located in this way in the full potential energy hypersurface was estimated using the Møller–Plesset perturbation theory up to second order.[15] The energy of such points was recalculated using the 6-31G** basis set.[16] $\Delta H°$, $\Delta S°$, and $\Delta G°$ values including zero-point energies also were calculated to obtain results more readily comparable to experiment. The partition functions provided by the statistical thermodynamic formulas within the ideal gas, rigid rotor, and harmonic oscillator approximations have been used for that purpose.[17] A pressure of 1 atm and a temperature of 298.15 K were assumed throughout.

Energetic minima were located by standard optimization methods, while transition states were located by the Schlegel algorithm.[18] It is well known that Schlegel's method requires a good starting point for the locating procedure. In the present study, a rather extensive search was needed to obtain a good approximation for the starting point. For that purpose, several internuclear distances were used as reaction coordinates, and energy profiles were generated. Transition-state locations were started at the maxima of these energetic profiles. Finally, it must be stressed that in all stationary points the Hessian matrix was checked to contain the right number of negative eigenvalues.

Results and Discussion

We present in this section the results obtained for the three reactions:

$$C_2H_4 + H_2 \rightarrow C_2H_6 \quad (1)$$

$$C_2H_4 + H_2 + HF \rightarrow C_2H_6 + HF \quad (2)$$

$$C_2H_4 + H_2 + H_3O^+ \rightarrow C_2H_6 + H_3O^+ \quad (3)$$

(4) (a) Zaera, F.; Somorjai, G. A. *J. Am. Chem. Soc.* **1984**, *106*, 2288. (b) Zaera, F.; Gellman, A. J.; Somorjai, G. A. *Acc. Chem. Res.* **1986**, *19*, 24-31.

(5) (a) Jardine, F. H.; Osborn, J. A.; Wilkinson, G.; Young, J. F. *Chem. Ind. (London)* **1965**, 560. (b) Bennett, M. A.; Longstaff, P. A. *Ibid.* **1965**, 846. (c) Osborn, J. A.; Jardine, F. H.; Young, J. F.; Wilkinson, G. *J. Chem. Soc. A* **1966**, 1711.

(6) (a) James, B. R. *Homogeneous Hydrogenation*; Wiley: New York, 1973. (b) Jardine, F. H. *Prog. Inorg. Chem.* **1981**, *28*, 63 and references therein.

(7) Dedieu, A. *Inorg. Chem.* **1980**, *19*, 375-383.

(8) (a) Wristers, J. *J. Am. Chem. Soc.* **1975**, *97*, 4312-4316. (b) Wristers, J. *Ibid.* **1977**, *99*, 5051-5055.

(9) Piner, H. *The Chemistry of Catalytic Hydrocarbon Conversions*; Academic Press: New York, 1981.

(10) (a) Saillard, J. Y.; Hoffmann, R. *J. Am. Chem. Soc.* **1984**, *106*, 2006-2026 and references therein. (b) Garcia-Prieto, J.; Ruiz, M. E.; Novaro, O. *Ibid.* **1985**, *107*, 5635-5644.

(11) (a) Dedieu, A.; Strich, A. *Inorg. Chem.* **1979**, *18*, 2940-2943. (b) Dedieu, A. *Ibid.* **1981**, *20*, 2803-2813.

(12) Binkley, J. S.; Frisch, M. J.; De Frees, D. J.; Krishnan, R.; Whiteside, R. A.; Schlegel, H. B.; Fluder, E. M.; Pople, J. A. GAUSSIAN 82, Carnegie-Mellon University, Pittsburgh, PA.

(13) Peterson, M. R.; Poirier, R. A. Program MONSTERGAUSS, Department of Chemistry, University of Toronto, Ontario, Canada, 1981.

(14) Binkley, J. S.; Pople, J. A.; Hehre, W. *J. Am. Chem. Soc.* **1980**, *102*, 939-947.

(15) (a) Møller, C.; Plesset, M. S. *Phys. Rev.* **1934**, *46*, 618. (b) Krishnan, R.; Pople, J. A. *Int. J. Quantum Chem.* **1978**, *14*, 91-100.

(16) Hariharan, P. C.; Pople, J. A. *Chem. Phys. Lett.* **1972**, *66*, 217.

(17) (a) Benson, S. W. *Thermochemical Kinetics*, 2nd ed.; Wiley-Interscience: New York, 1976. (b) Lewis, G. N.; Randall, M. *Thermodynamics*; Pitzer, K. S., Brewer, L., Eds; McGraw-Hill: New York, 1961; pp 419-448. (c) Kinox, J. H. *Molecular Thermodynamics*; Wiley: New York, 1978; pp 95-143.

(18) Schlegel, H. B. *J. Comput. Chem.* **1982**, *3*, 214-218.

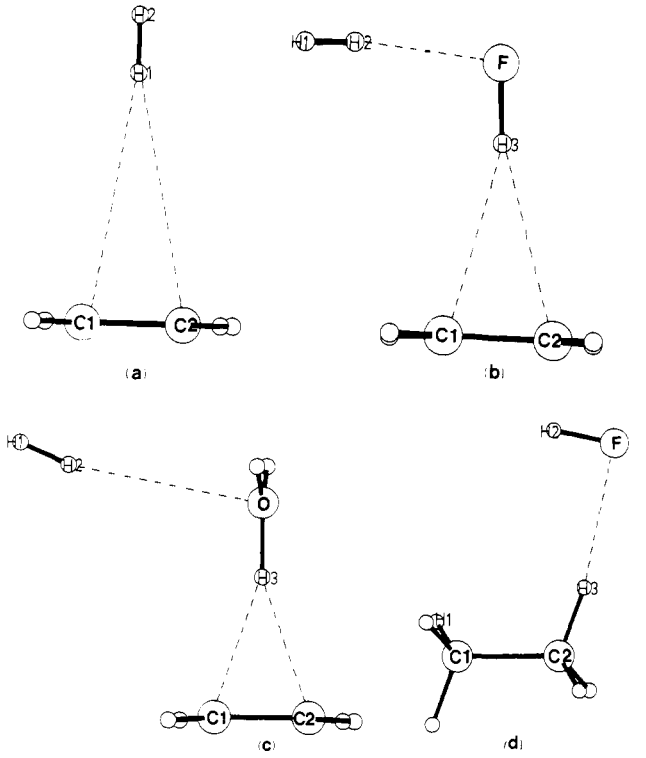

Figure 1. 3-21G optimized structures of the following complexes: (a) $C_2H_4 \cdot H_2$, (b) $C_2H_4 \cdot HF \cdot H_2$, (c) $C_2H_4 \cdot H_3O^+ \cdot H_2$, (d) $C_2H_6 \cdot HF$.

where (1) corresponds to the addition of hydrogen to ethylene, and (2) or (3) corresponds to the same reaction (1) catalyzed by two different acids, either hydrofluoric acid in (2), or hydronium ion in (3). Since this paper is aimed to get an insight into the catalytic action in ethylene hydrogenation, results for the three reactions will be presented together. First of all, the optimized structures of reactants, products, and transition states will be given. Secondly, the energy profiles of the three reactions will be calculated starting from these structures, followed by an analysis of thermodynamic results. Finally, an insight into the catalytic action will be performed.

Structures of Reactants and Products. In Table I we summarize the most relevant geometrical parameters of the optimized reactants and products of reactions 1–3. In Figure 1 the reactants for the three reactions are also depicted. The initial $C_2H_4 \cdot H_2$ complex (Figure 1a) presents a C_{2v} symmetry where the H–H bond distances are almost unchanged with respect to ethylene and hydrogen. Both HF and H_3O^+ also form C_{2v}-symmetry complexes with ethylene, but the distances between the hydrogen atom in the acid and the midpoint of the C–C bond are a little shorter. The C–C and H–X bond lengths are in turn lengthened. The structures of these two complexes agree with the results appeared in the literature for the $C_2H_4 \cdot HF$ and $C_2H_4 \cdot H_3O^+$ complexes.[19,20] The termolecular complexes $C_2H_4 \cdot HF \cdot H_2$ and $C_2H_4 \cdot H_3O^+ \cdot H_2$ that are the reactant complexes of reactions 2 and 3, respectively, are displayed in Figure 1b and 1c. From inspection of Table I, one can see that they resemble closely the $C_2H_4 \cdot HF$ and $C_2H_4 \cdot H_3O^+$ complexes, where the hydrogen molecule is bonded to the acid fragment and represents just a small perturbation of the ethylene–acid system. This tiny perturbation agrees perfectly with the well-known fact stated in the literature that complexes between HF or H_3O^+ and molecular hydrogen are loosely bound.[21,22]

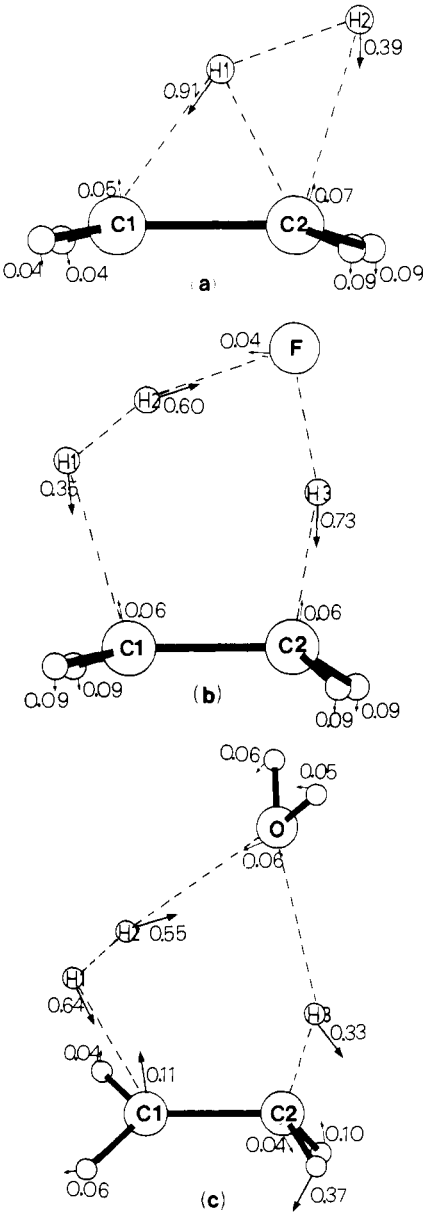

Figure 2. 3-21G optimized structures for the transition states of reactions 1 (TS1, a), 2 (TS2, b), and 3 (TS3, c). Arrows indicate the main components of the transition vector.

As a final product of reactions 1–3 alternating ethane is obtained in all cases. In reactions 2 and 3, a new acid molecule is formed from a hydrogen atom formerly belonging to the hydrogen molecule. This acid molecule stays complexed with ethane, as can be seen in Figure 1d for the HF-catalyzed reaction 2.

Structures of Transition States. The main geometrical parameters of the three transition states corresponding to reactions 1 to 3 are collected in Table I, and their appearance is depicted in Figure 2, together with the meaningful components of their transition vector. These transition states will be referred to as TS1, TS2, and TS3 from now on. Regarding reaction 1, the transition state TS1 (Figure 2a) has the hydrogen molecule and the two carbon atoms in the same plane. Furthermore inspection of the transition vector shows clearly that the reaction proceeds toward formation of ethane. The structure of TS1 resembles the 6-31G* transition state found earlier by Pople et al. for the same reaction.[2] The present study with the 3-21G basis set shows that the hydrogen molecule lies farther from ethylene, and that the

(19) (a) Del Bene, J. E. *Chem. Phys. Lett.* **1974**, *24*, 203–207. (b) Pople, J. A.; Frisch, M. J.; Del Bene, J. E. *Ibid.* **1982**, *91*, 185–189. (c) Volkmann, D.; Zuranski, B.; Heidrich, D. *Int. J. Quantum Chem.* **1982**, *22*, 631–637. (d) Sapse, A. M.; Jain, D. C. *J. Phys. Chem.* **1984**, *88*, 4970–4973.

(20) (a) Cao, H. Z.; Allavena, M.; Tapia, O.; Evleth, E. M. *Chem. Phys. Lett.* **1983**, *96*, 458–463. (b) Jones, W. H.; Mariani, R. D.; Lively, M. L. *Ibid.* **1984**, *108*, 602–608. (c) Jones, W. H.; Mezey, P. G.; Csizmadia, I. G. *THEOCHEM* **1985**, *22*, 85–92.

(21) Bernholdt, D. E.; Liu, S.; Dykstra, C. E. *J. Chem. Phys.* **1986**, *85*, 5120–5126.

(22) Okumura, M.; Yeh, L. I.; Myers, J. D.; Lee, Y. T. *J. Chem. Phys.* **1986**, *85*, 2328–2329.

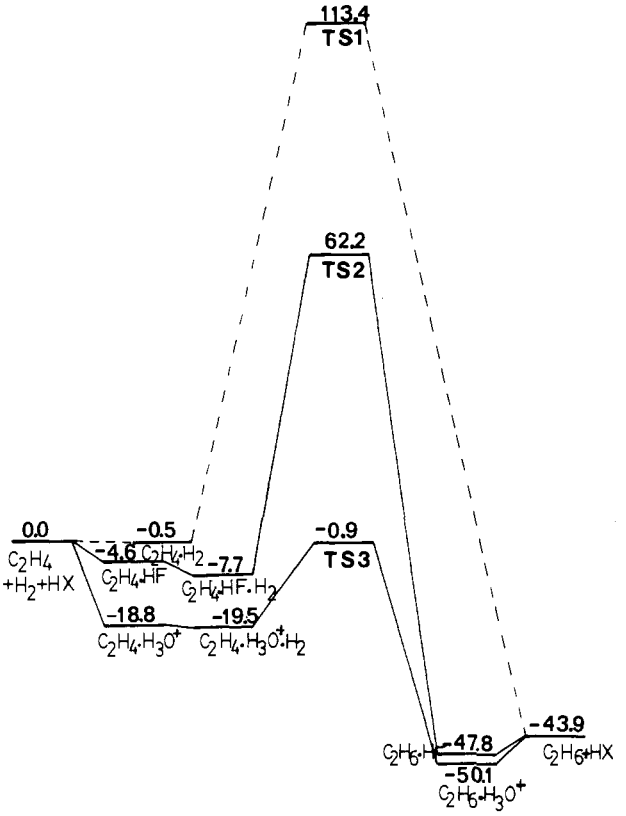

Figure 3. Relative 3-21G potential energies for the uncatalyzed reaction 1, and for the HF- and H_3O^+-catalyzed reactions 2 and 3. Energies are given in kcal/mol.

H–H bond length is shorter than in the structure found by Pople.

The transition states for reactions 2 TS2 (Figure 2b) and 3 TS3 (Figure 2c) exhibit a cyclic six-center structure that contains both carbon atoms, the hydrogen molecule, the fluorine or oxygen atom, and the hydrogen of the acid. One difference appears between both termolecular transition states: in TS2 a plane contains the six-membered ring, whereas in TS3 the ring is not contained in a single plane. Comparison of Figures 2b and 2c with the corresponding reactants in Figures 1b and 1c shows also that the hydrogen molecule is placed in a suitable position to react with ethylene. On the contrary, the two reactant complexes present the hydrogen molecule pulled apart from ethylene. If we look at the meaningful components of both transition vectors displayed in Figure 3 as well, we may determine what geometrical parameters define the reaction coordinate at the transition state. For reaction 2, one can see that the main motions correspond to a hydrogen transfer from fluorine to carbon, and a simultaneous transfer of a hydrogen to fluorine and another hydrogen to ethylene that produces the rupture of the hydrogen molecule. Therefore hydrogen fluoride acts as a bifunctional catalyst, because it transfers the acidic proton to ethylene, while it accepts a proton from the hydrogen molecule. With regard to TS3, since not all atoms lie in the same plane and there are several meaningful out-of-plane components, interpretation of the reaction coordinate is not quite so easy, although the three motions that appear in TS2 can also be detected.

If the three transition states are compared, one can see that the hydrogen molecule is broken more in TS1 than in TS2, whereas TS3 exhibits an almost undistorted hydrogen molecule. One can say also that the proton transfer is far more advanced in TS3 than in TS2. This fact, together with the longer H–H bond in TS2 than in TS3, indicates that the mechanism of the HF reaction 2 is more concerted than that of the H_3O^+ process 3.

Energetics. Using the optimized 3-21G structures described above, we have calculated the total energies of the species involved in the three reactions. Single-point calculations including either correlation energy at the MP2 level, or the larger 6-31G** basis set, have been also performed. These absolute energies, together with zero-point energies, are collected in Table II. The energies relative to separated reactants are given in Table III, while in Figure 3 we present an energetic diagram obtained from the 3-21G SCF energies.

Table II. 3-21G SCF, 6-31G** SCF, and MP2/3-21G Total Energies along with 3-21G Zero-Point Energies for Reactants, Transition States, and Products of Reactions 1–3[a]

	HF/3-21G //3-21G	ZPE	MP2/3-21G //3-21G	HF/6-31G** //3-21G
C_2H_4	−77.600 99	34.6	−77.783 36	−78.038 81
H_2	−1.122 96	6.7	−1.140 22	−1.131 31
HF	−99.460 22	5.8	−99.583 44	−100.010 06
H_3O^+	−75.891 23	22.0	−76.018 85	−76.307 67
C_2H_4·H_2	−78.724 76	42.3	−78.924 60	−79.170 72
TS1	−78.543 23	42.4	−78.748 47	−79.005 94
C_2H_6	−78.793 95	50.2	−78.984 82	−79.238 08
C_2H_4·HF	−177.068 60	42.0	−177.374 29	−178.055 30
C_2H_4·HF·H_2	−178.196 40	51.1	−178.521 52	−179.187 38
TS2	−178.085 12	52.6	−178.424 10	−179.058 32
C_2H_6·HF	−178.260 29	57.3	−178.577 17	−179.248 31
C_2H_4·H_3O^+	−153.522 21	58.1	−153.834 21	−154.374 62
C_2H_4·H_3O^+·H_2	−154.646 18	65.6	−154.976 05	−155.505 84
TS3	−154.616 56	67.5	−154.930 94	−155.491 53
C_2H_6·H_3O^+	−154.695 07	73.1	−155.016 07	−155.553 47

[a] Electronic energies are in a.u., zero-point energies (ZPE) in kcal/mol.

Table III. Energies (in kcal/mol) Relative to Separated Reactants for the Different Species Involved in Reactions 1–3

	ΔESCF1[a]	$\Delta\Delta E_0$[b]	ΔΔEMP2[c]	ΔE_{tot}[d]	ΔESCF**[e]
C_2H_4 + H_2 + HX[f]	0	0	0	0	0
C_2H_4·H_2	−0.5	1.0	−0.1	0.4	−0.4
C_2H_4·HF	−4.6	1.6	−0.1	−3.1	−4.0
C_2H_4·HF·H_2	−7.7	4.0	−2.7	−6.4	−4.5
C_2H_4·H_3O^+	−18.8	1.5	−1.3	−18.6	−17.7
C_2H_4·H_3O^+·H_2	−19.5	2.3	−1.6	−18.8	−17.6
TS1	113.4	1.1	−3.5	111.0	103.0
TS2	62.2	5.5	−11.4	56.3	76.5
TS3	−0.9	4.2	8.1	11.4	−8.6
C_2H_6·HF	−47.8	10.2	3.8	−33.8	−42.7
C_2H_6·H_3O^+	−50.1	9.8	7.3	−33.0	−47.5
C_2H_6	−43.9	8.9	5.5	−29.5	−42.6

[a] HF/3-21G//3-21G relative energies. [b] Corrections arising from ZPE at the HF/3-21G level. [c] Corrections arising from correlation energy at the MP2/3-21G//HF/3-21G level. [d] ΔE_{tot} = ΔESCF1 + $\Delta\Delta E_0$ + ΔΔEMP2. [e] HF/6-31G**//3-21G relative energies. [f] X = F for reaction 2 and X = OH_2^+ for reaction 3.

We can see in Figure 3 that at the 3-21G SCF level the potential energy barrier is lowered to 62.2 kcal/mol when the reaction is catalyzed by HF, down from 113.4 kcal/mol for the uncatalyzed process. When the catalyst is H_3O^+, the barrier goes down even more dramatically, such that the transition state lies 0.8 kcal/mol under the separated reactants. If the trimolecular reactant complexes of Figure 1a–c are taken as zeroes of energy, the computed energy barrier values become 113.9, 69.9, and 18.6 kcal/mol for the uncatalyzed, HF- and H_3O^+-catalyzed processes, respectively. One finds again that the barrier height is lowered owing to the acid catalysis, and that this decrease is closely related to the acid strength. Another fact arises from Figure 3: a stabilization due to the formation of the ethylene–acid complexes is achieved, and a small additional stabilization is produced by the formation of the termolecular reactant complexes. Likewise, the product complexes of the termolecular additions are lower in energy than the separated products, ethane plus acid.

The foregoing results at the 3-21G SCF level may exhibit three shortcomings: first of all, zero-point energies are not included. Second, the correlation energy is missing. Finally, the basis set may be too small. To overcome these possible shortcomings, we have corrected the 3-21G SCF energies for the three of them. The correlation energy has been included, without any geometry reoptimization, with the aid of Møller–Plesset perturbation theory up to second order, while the basis set size has been augmented by using the 6-31G** basis set. From inspection of Tables II and III, it can be seen that zero-point energies have little influence on barrier heights, although they have a noticeable effect on the exothermiticity of the reaction, which is decreased by about 10

Table IV. Contributions to $\Delta G°$ Relative to Separated Reactants for the Different Species Involved in Reactions 1–3

	ΔE^a	$\Delta E_t^{a,c}$	ΔH^a	ΔS^b	$-T\Delta S^a$	ΔG^a
$C_2H_4 + H_2 + HX^d$	0.0	0.0	0.0	0.0	0.0	0.0
$C_2H_4 \cdot H_2$	−0.5	1.7	0.6	−9.64	2.9	3.5
$C_2H_4 \cdot HF$	−4.6	1.9	−3.3	−19.85	5.9	2.6
$C_2H_4 \cdot HF \cdot H_2$	−17.7	4.3	−4.6	−36.14	10.8	6.2
$C_2H_4 \cdot H_3O^+$	−18.8	1.5	−17.9	−23.78	7.1	−10.8
$C_2H_4 \cdot H_3O^+ \cdot H_2$	−19.5	3.2	−17.5	−32.31	9.6	−7.9
TS1	113.4	−0.1	112.9	−25.90	7.7	120.6
TS2	62.2	3.4	64.4	−59.38	17.7	82.1
TS3	−0.9	3.3	1.2	−53.80	16.0	17.2
$C_2H_6 \cdot HF$	−47.8	9.7	−39.3	−43.57	13.0	−26.3
$C_2H_6 \cdot H_3O^+$	−50.0	9.4	−41.8	−43.73	13.0	−28.8
C_2H_6	−43.9	7.9	−36.6	−28.92	8.6	−28.0

[a] In kcal/mol. [b] In eu. [c] Thermal energies including zero-point energy and vibrational excited states and rotational contributions. [d] X = F for reaction 2 and X = OH_2^+ for reaction 3.

kcal/mol. With respect to correlation energy, it has a random effect. Whereas the barrier for reaction 2 is decreased, and the barrier for reaction 1 is lowered slightly, the height for the H_3O^+-catalyzed process 3 is increased. The exothermicities of the three reactions decrease in all cases, although not to such an extent as in the zero-point energy correction. If both zero-point and correlation energy corrections are considered, it can be observed that the gap between the uncatalyzed and catalyzed processes is increased. On the contrary, the barrier heights of the two catalyzed reactions approach each other. The most noticeable fact is found in exothermicities that are decreased to a large extent. If attention is drawn to increase of the basis set size, the difference in barrier heights between the uncatalyzed and catalyzed processes diminishes, while the difference between the two acid-catalyzed processes increases. Moreover, the exothermicities are decreased only slightly. If the effect due to the correlation energy and that due to the basis set size are compared, one can see that at the transition-state geometries the energy changes in the computed barriers go in opposite directions and may be somewhat offset. Some cancellation of correlation and basis set size corrections are also found in different chemical reactions.[23]

In order to discuss the results obtained for the three reactions, mention must be made that only the uncatalyzed process has been subject of a recent theoretical study and has some experimental data available for its heat of reaction. Our value for the transition-state barrier of reaction 1 at the 3-21G SCF level, 113.4 kcal/mol, is higher than the value obtained by Pople et al. with the 6-311G** basis set (100.9 kcal/mol).[2] However, our value using the larger 6-31G** basis set (103.0) is much closer to their SCF value. Regarding exothermicity, our 3-21G SCF computed value overestimates it. Nevertheless, inclusion of correlation energy and zero-point energy corrections approach our results (−29.5 kcal/mol) to the experimental value (−34.7 kcal/mol).[24]

Although the results presented in Figure 3 may be subject to change due to zero-point energies, correlation energy, or basis set size, quantitative changes are always small when compared to barrier height differences. Therefore, any qualitative conclusions based on 3-21G SCF results seem to be reliable.

Thermodynamic Analysis. It is clear that in calculations involving such ordered structures as the ones dealt with in this paper, energetic considerations are somewhat doubtful, because entropic contributions may be of the same order as energetic ones. A thermodynamical analysis is thus needed to fully support the conclusions reached on an energy basis.

In Table IV we present the various contributions to $\Delta G°_{298}$ for the three reactions studied in this paper. In addition, Figure 4 shows a diagram of the $\Delta G°_{298}$ relative values for reactions 1 to 3.

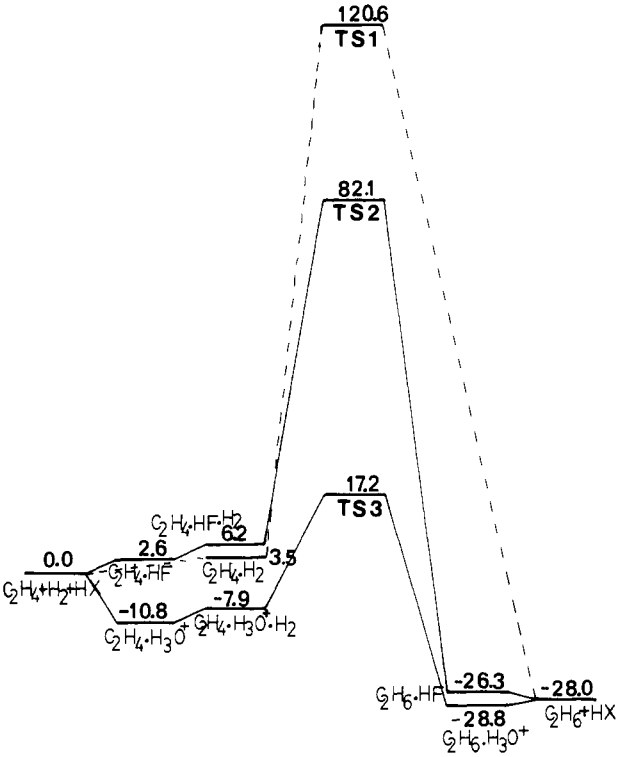

Figure 4. Relative 3-21G Gibbs free energies for the uncatalyzed reaction 1, and for the HF- and H_3O^+-catalyzed reactions 2 and 3. Energies are given in kcal/mol.

The most noteworthy fact is that the entropic term is far more important in termolecular processes 2 and 3 than in the bimolecular process 1, as can be expected from the higher degree of ordering of the former processes. It is also interesting to note that the $C_2H_4 \cdot H_2$ and $C_2H_4 \cdot HF \cdot H_2$ reactant complexes are not stable from a free-energy analysis, whereas the $C_2H_4 \cdot H_3O^+ \cdot H_2$ reactant complex is stable even in a free-energy scale. The barriers to molecular hydrogen addition do not change meaningfully from Figure 3: catalyzed processes 2 and 3 are very favored compared to the uncatalyzed process 1, and energy barrier heights are heavily dependent on the acid strength.

Catalytic Action. We have shown above that there is a large catalytic action by the acids in reactions 2 and 3. The aim of this section is to provide a deeper insight into the mechanism of such a catalytic action. A first analysis has been performed already starting from the geometrical parameters of the transition states of the three reactions. To discuss quantitatively the degree of formation and rupture of the bonds that make up the four- and six-membered rings of the transition states and reactant or product complexes, a bond-order concept has been employed, since the bond lengths in the transition states are intermediate between their reactant and product values. For this purpose we have used the Pauling bond orders[25] that have been shown to be very useful in similar reactions.[26] A Pauling bond order is defined as

$$B = \exp\{[R(1) - R(B)]/0.3\} \quad (4)$$

where $R(1)$ is a bond length in separated reactants or products that is assigned order one, and $R(B)$ is the length of such bond in the considered structure. In Table V we collect the Pauling bond orders for the species that intervene in reactions 1 to 3. Special interest merits the H1–H2 bond order, because its rupture accounts for a large part of potential energy barriers. One can see that in the reactant complexes the bond orders are one, while in the product complexes they are zero or almost zero. At the transition states, the H1–H2 bond order has an intermediate value,

(23) Oie, T.; Loew, G. H.; Burt, S. K.; Binkley, J. S.; MacElroy, R. D. *Int. J. Quantum Chem., Quantum Biol. Symp.* **1982**, *9*, 223–245.
(24) (a) Stull, D. R.; Prophet, H., Eds. *JANAF Thermochemical Tables*; NSRDS-NBS: Washington, D.C., 1971; p 37. (b) Chase, M. W., Cornutt, J. L.; Downey, J. R.; McDonald, R. A.; Severod, A. N.; Valenzuela, E. A. *J. Phys. Chem. Ref. Data* **1982**, *11*, 695.
(25) Pauling, L. *J. Am. Chem. Soc.* **1947**, *69*, 542–553.
(26) (a) Williams, I. H.; Spangler, D.; Maggiora, G. M.; Schowen, R. L. *J. Am. Chem. Soc.* **1985**, *107*, 7717–7723. (b) Yamataka, H.; Tamura, S.; Ando, T.; Hanafusa, T. *Ibid.* **1986**, *108*, 601–606.

Table V. Pauling Bond Orders for the Different Species that Intervene in Reactions 1–3

	C1–C2	H1–C1	H1–H2	H2–C2	H2–X	X–H3	H3–C2
$C_2H_4 \cdot H_2$	1.00	0.00	1.00				
$C_2H_4 \cdot HF$	0.98					0.99	0.01
$C_2H_4 \cdot HF \cdot H_2$	0.98	0.00	1.00		0.02	0.98	0.01
$C_2H_4 \cdot H_3O^+$	0.95					0.85	0.04
$C_2H_4 \cdot H_3O^+ \cdot H_2$	0.95	0.00	1.00		0.00	0.85	0.04
TS1	0.69	0.27	0.23	0.13			
TS2	0.73	0.56	0.65		0.25	0.37	0.45
TS3	0.62	0.06	0.93		0.04	0.03	0.97
$C_2H_6 \cdot HF$	0.47	1.00	0.00		1.00	0.02	1.01
$C_2H_6 \cdot H_3O^+$	0.46	0.98	0.02		0.97	0.00	0.99
C_2H_6	0.47	1.00	0.00	1.00			1.00

quite small for (1), intermediate for (2), and almost one for (3). Hence, the hydrogen molecule is almost completely broken in TS1, whereas it has just begun to break in TS3. It can now be seen that the energy barriers for (1), (2), and (3) are related to the H–H bond order: the smaller the bond order, the higher the barrier. The C1–C2 bond order, i.e., the change from ethylene to ethane, is quite constant along the three reactions and decreases when going from reactants to products. Concerning the H1–C1 bond order, it increases when going from reactants to products. In transition states, it is worth noting that its value for (2) is much higher than for (1), and that for (3) is close to zero. That means that, while in TS2 the H1–C1 bond is halfway formed, in TS3 it has just begun its formation. Something similar can be said about the H2–X bond order, though the value for (2) is almost half of the H1–C1 bond order value. Special attention must be paid to the X–H3 and H3–C2 bond orders: when the reaction advances, the first one decreases and the second one increases. At the trimolecular transition states they behave in a different way: whereas in TS2 they have a close value, in TS3 X–H3 is almost zero and H3–C2 is almost one. In other words, transfer of the proton is already achieved in TS3, whereas it is halfway done in TS2.

If we take into account the whole set of data for reactions 2 and 3, one can see that all bond orders that correspond to atoms of the six-membered ring exhibit intermediate values between reactants and products. Therefore, the concerted character of this process emerges clearly. On the contrary, for TS3 it appears that the acidic hydrogen has been almost completely transferred, the hydrogen molecule is fully bonded, and the H1–C1 and H2–X bonds begin to be formed. Hence, reaction 3 exhibits a two-phase character, where the first phase consists of a proton transfer and formation of a carbocation. Really, the charge of the $C_2H_5^+$ fragment is 0.80 eu, which is obviously much larger than the value of 0.42 eu for TS2.

The differences pointed above between both termolecular transition states can also be seen starting from an analysis of the charge density maps. For TS2, we have represented in Figure 5a the density map in the plane of the six-center ring. For TS3, the six-membered ring atoms are not coplanar, so we have chosen a plane as close as possible to the six atoms. The charge density map in this plane is plotted in Figure 5b. The critical points of the charge density (bond and ring critical points in the terminology of Bader[27]) are also shown in this Figure. A first striking aspect of both a and b in Figure 5 is the appearance of a ring critical point that confirms the formation of a six-membered ring. Further, the most noticeable difference arises from the electronic density around H3, which is the hydrogen atom being transferred from the acid to ethylene. In TS2, H3 is being halfway transferred from the acid to ethylene, as shown by the equal values of the H3–F and H3–C bond critical point densities. On the contrary, in TS3 H3 has been completely transferred, because the value of the H3–C bond critical point density is very low, and the hydrogen atom is incorporated into a $C_2H_5^+$ fragment. Another fact arises from Figure 5a: fluorine is somewhat bonded to H2, while H1 is being bonded to C1. Hence, the concerted character of reaction 2 shows up clearly. On the contrary, it can be easily seen from Figure 5b that O1 and C1 are very loosely bonded to the hydrogen molecule, so that the two-phase character of reaction 3 appears again.

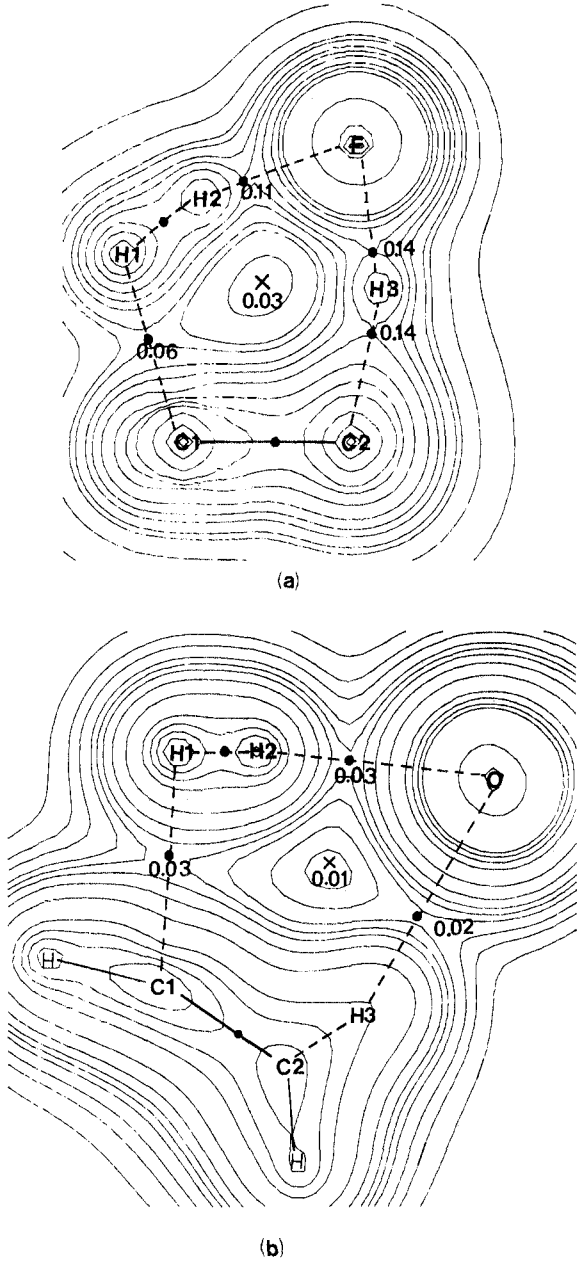

Figure 5. Charge density plots (see text for details) for the trimolecular transition state of 2 (TS2, a) and 3 (TS3, b): ● indicates bond critical points, × indicates ring critical points, and numbers indicate electronic density at these points. Bond paths linking atoms are also shown.

The preceding analysis suggests clearly that the acid catalysis of ethylene hydrogenation proceeds via the formation of a six-

(27) Bader, R. F. W.; Tal, Y.; Anderson, S. G.; Nguyen-Dang, T. T. *Isr. J. Chem.* **1980**, *19*, 8–29 and references therein.

membered ring which involves both carbons of ethylene, the hydrogen molecule, the oxygen or fluorine atom, and the acidic proton. Several common points have to be stressed: a proton must be transferred from the acid toward ethylene; the hydrogen molecule breaks and forms a hydride ion, and a proton is subsequently formed to generate the initial acid molecule. However, differences between a normal acid and a strong acid arise in reactions 2 and 3. In (2), catalyzed by HF, there is a bifunctional catalysis and the process is very concerted. The acid acts as a catalyst that simultaneously releases and accepts a proton. In this way, the acid contributes to the breakage of the hydrogen molecule. Similar bifunctional catalysis have been theoretically studied and reported in the literature for analogous processes.[28] In contrast to (2), in reaction 3, catalyzed by a strong acid such as H_3O^+, the first phase of the process consists of the full proton transfer from the acid to ethylene to form the carbocation. Not until a second phase is the hydrogen molecule broken owing to the action of the existing carbocation, helped by the conjugated base of the acid. This mechanism is almost coincident with the mechanism proposed from experimental data, where a carbocation is formed in a first step, and a hydride ion attacks later the carbocation to form the alkane.[8a] Our mechanism for reaction 3 is distinguished from the experimentally proposed mechanism in that, although a carbocation is formed initially, the mechanism does not proceed through two steps but via an unique step with two phases.

If we compare the acid catalysis as described in this paper with the heterogeneous or homogeneous catalysis by metals, a remarkable difference exists. Whereas metal catalysis implies breakage of the hydrogen molecule as a first step, the acid catalysis in reaction 3 requires the formation of the carbocation in the first phase. The catalysis by normal acids such as HF (eq 2) exhibits an intermediate behavior, because the hydrogen molecule rupture and the carbocation formation are simultaneously done, as seen in the concertedness of the reaction.

A last aspect of the two acid-catalyzed reactions studied in this paper is their possibility of being carried out experimentally. With respect to the catalysis by hydrogen fluoride, it is clear that it implies a high internal energy barrier that will make the actual reaction quite difficult. Furthermore, a competitive reaction exists that involves entrance of HF instead of H_2 into ethylene and proceeds via a lower energy barrier.[29] Finally, the reactant complexes C_2H_4·HF and C_2H_4·HF·H_2 have $\Delta G°_{298} > 0$, so that their population with respect to separated species will be minimal. On the contrary, catalysis of ethylene hydrogenation by H_3O^+ seems to be very favorable from either, the low computed energy barrier and the free-energy stability of the reactant complex C_2H_4·H_3O^+·H_2. This complex can be easily generated by a collision of the very favorable complex C_2H_4·H_3O^+ and a hydrogen molecule. It is clear that other reactions like the acid-catalyzed formation of alcohols may compete with hydrogenation, but certain experimental conditions may be chosen so that hydrogenation becomes the main reaction.

Conclusions

In the present work we have theoretically studied the acid catalysis of olefin hydrogenation reactions. Ethylene has been chosen as a model for olefin, while HF and H_3O^+ have been chosen as models for normal and strong acids, respectively. Whereas catalysis by a normal acid shows bifunctional characteristics and does not seem to be very efficient, catalysis by a strong acid exhibits special characteristics such that, given an adequate choice of experimental conditions, it may be an adequate way to hydrogenate olefins. Existing experimental data on the acid-catalyzed hydrogenation of aromatic compounds show the feasibility of this type of reactions, which in our opinion are worth further experimental research effort.

Acknowledgment. This work has been supported by the Spanish "Comisiõn Asesora de Investigaciõn Cientifica y Técnica" under Contract No. 3344/83.

Registry No. CH_2=CH_2, 74-85-1; HF, 7664-39-3; H_3O^+, 13968-08-6.

(28) (a) Ruelle, P.; Kesselring, U. W.; Nam-Tram, H. *J. Am. Chem. Soc.* **1986**, *108*, 371-375. (b) Clavero, C.; Duran, M.; Lledõs, A.; Ventura, O. N.; Bertrán, J. *Ibid.* **1986**, *108*, 923-928.

(29) Kato, S.; Morokuma, K. *J. Chem. Phys.* **1980**, *73*, 3900-3914.

Theoretical Calculations on Adenine and Adenosine and Their 8-Chloro-Substituted Analogues

Gerald A. Walker,[†,‡] Subhash C. Bhatia,[‡] and John H. Hall, Jr.*[‡,⊥]

Contribution from the Department of Chemistry, Atlanta University, Atlanta, Georgia 30314, Dolphus E. Milligan Science Research Institute, Atlanta University Center Inc., Atlanta, Georgia 30310, and the School of Geophysical Sciences, Georgia Institute of Technology, Atlanta, Georgia 30332. *Received March 26, 1987*

Abstract: Ab initio STO-3G level calculations and localized molecular orbitals from the partial retention of diatomic differential overlap method are reported for various protonated and tautomeric forms of adenine. The localized molecular orbitals indicate that the bonding patterns of the electrons are highly sensitive to the protonated site, consistent with experimental results. Calculation of the conformational energies of adenosine shows that N_3-protonation is more favorable in the anti conformation than N_3 protonation in the syn conformation by 32.2 kcal/mol. Our calculations also indicate that N_3-protonation may cause a change in conformation. The calculations for 8-chloroadenosine show a higher rotational barrier about the base–ribose bond than the rotational barriers obtained for adenosine and N_3-protonated adenosine.

Many different approaches[1] have been used to determine the underlying mechanisms related to the function of DNA and RNA in biological systems. One approach has been to examine the chemistry of their basic units in relation to the behavior of the macromolecular structures in attempts to explain the experimental data.[2] Since it is extremely difficult to experimentally determine the atomic interactions in enzymes and macromolecular systems, theoretical techniques have been very useful for studying reaction mechanisms in biological systems.[3]

[†] Atlanta University.
[‡] Atlanta University Center Inc.
[⊥] Georgia Institute of Technology.

(1) Saenger, W. *Principles of Nucleic Acid Structure*; Springer-Verlag: New York, 1974; Chapter 3.
(2) Reference 1; Chapter 1.

0002-7863/87/1509-7629$01.50/0